Bioenergetic and Mechanical Modeling of Endurance Sports with Emphasis on Individualization

Julius Lidar

Main supervisors: Prof. Mikael Bäckström
Co-supervisors: Assoc. Prof. Mats Ainegren, Dr. David Sundström

Sports Tech Research Centre
Department of Engineering, Mathematics and Science Education
Faculty of Science, Technology and Media
Thesis for Licentiate degree in Technology
Mid Sweden University
Östersund, Sweden, 2023-02-28

Akademisk avhandling som med tillstånd av Mittuniversitetet i Östersund framläggs till offentlig granskning för avläggande av teknologie licentiatexamen måndag, 2023-04-03, 13:15, Q221, Mittuniversitetet Östersund. Seminariet kommer att hållas på engelska.

Bioenergetic and Mechanical Modeling of Endurance Sports with Emphasis on Individualization

Printed by Mid Sweden University, Sundsvall, Sweden

ISSN: 1652-8948

ISBN: 978-91-89786-04-2

Faculty of Science, Technology and Media
Mid Sweden University, SE-831 25, Östersund, Sweden
Phone: +46 (0)10 142 87 03

Mid Sweden University Licentiate Thesis 194

To my father, the kindest of them all. When you were forced to leave us, my path was still uncertain. I believe you would have been intrigued and proud of my journey and my work, even though I know you would have supported any choices I made.

Acknowledgement

I would like to express my sincere gratitude to my supervisors Mikael Bäckström, Mats Ainegren, and David Sundström for their unwavering support, invaluable discussions, and collaborative efforts throughout the duration of this thesis. They have always been willing to lend a helping hand or thought, and their genuine interest in my work has been greatly appreciated. Additionally, I would like to extend my thanks to Erik Andersson for his fruitful collaboration on Paper II.

I would also like to acknowledge all my colleagues at Sports Tech Research Centre for their positivity and willingness to assist with any challenges, no matter how big or small. Finally, I would like to express my heartfelt appreciation and love to my family Blenda, Fridolf, and Emma. You are the golden core of my life who help me keep track of what is really, truly important.

Table of contents

Abstract

Endurance athletes strive to improve their race times by enhancing their physical abilities, techniques, tactics, and equipment. Numerical simulations can aid in this effort by enabling repeated testing under identical conditions, thus isolating the effect of a single variable of interest on race time. This thesis outlines the mechanical assumptions and mathematical formulations to conducting numerical simulations. Paper I exemplifies applications and limitations when using numerical simulations with a propulsive power model, by investigating the impact of dynamic friction on race times in cross-country skiing.

Further, the thesis introduces bioenergetic modeling as a possible method for more accurately modeling an athlete's propulsive power. It provides an overview of existing bioenergetic models and describes a non-linear grey-box parameter estimation method for individualizing bioenergetic model formulations to reflect an individual athlete's bioenergetic systems. In Paper II, an assessment of validation for two existing bioenergetic models is performed on an individual level when applied to simulated sprint time trials in cross-country skiing. The models show overall good agreement with measurement data but lack the ability to capture the dynamics of the human metabolic energy systems in more detail.

In Paper III, a new bioenergetic model is developed which describes the dynamic behavior of the metabolic energy supply systems and various sources of metabolic demand. The model is individualized and validated against intermittent cycling with varying power output. Although the model shows good agreement with measurements, it does not capture the details of the aerobic slow component and periods of recovery, indicating a need for continued development.

Summary in Swedish

Uthållighetsidrottare strävar efter att korta sina tävlingstider genom förbättrad fysisk förmåga, teknik, taktik och utrustning. Numeriska simuleringar kan hjälpa till i detta arbete genom att möjliggöra upprepade tester med identiska förhållanden där inverkan från en enskild variabel på tävlingstiden isoleras. Denna avhandling beskriver de mekaniska antaganden och matematiska formuleringar som krävs för att utföra numeriska simuleringar. Artikel I exemplifierar tillämpningar och begränsningar för simuleringar i kombination med en empirisk modell för framdrivande effekt genom att undersöka den dynamiska friktionens inverkan på tävlingstider i längdskidåkning.

Avhandlingen introducerar bioenergisk modellering som en möjlig metod för att mer exakt modellera en idrottares uteffekt. Vidare ges en översikt över befintliga bioenergiska modeller och en metod för att anpassa bioenergiska modeller till att återspegla en specifik idrottares metabola system. I Artikel II utförs en utvärdering av validiteten för två befintliga bioenergiska modeller på individnivå när de tillämpas på simulerade sprintlopp i längdskidåkning. Modellerna visar överlag god överensstämmelse med mätdata, men saknar förmågan att fånga detaljerna i de mänskliga metaboliska energisystemens dynamik.

I Artikel III utvecklas en ny bioenergisk modell som beskriver dynamiken hos de metabola energiförsörjningssystemen och flera processer som ger upphov till metabola krav. Modellen individanpassas och valideras mot intermittent cykling med varierande uteffekt. Modellen visar god överensstämmelse med mätdata, men lyckas inte fånga detaljerna i det aeroba systemet vid de högsta uteffekterna eller vid perioder av återhämtning, vilket motiverar fortsatt utveckling.

List of papers

This thesis is mainly based on the following three papers, herein referred to by their corresponding Roman numerals:

Paper I *Impact of dynamic friction on race times in cross-country skate skiing – a numerical simulation study.*
J. Lidar, D. Sundström, M. Ainegren
European College of Sport Science Virtual Congress, 26th ECSS Anniversary Congress, 2021, 8-10 September
Author contribution: As first author, Julius Lidar was the main contributor in designing and conducting the study and writing the manuscript.

Paper II *Validity and Reliability of Hydraulic-Analogy Bioenergetic Models in Sprint Roller Skiing*
J. Lidar, E. P. Andersson, D. Sundström
Frontiers in Physiology, Vol. 12.
DOI: 10.3389/fphys.2021.726414
Author contribution: As first author, JL was the main contributor in designing and conducting the study and writing the manuscript. JL did not contribute to the experimental data collection or statistical calculations.

Paper III *Development and Validation of Dynamic Bioenergetic Model for Cycling*
J. Lidar, M. Ainegren, D. Sundström
Submitted manuscript
Author contribution: As first author, Julius Lidar was the main contributor in designing and conducting the study and writing the manuscript. MA was the main responsible for the clinical data collection.

List of symbols and abbreviations

2TM	two-tank model (Paper II)
3TM	three-tank model (Paper II)
A	projected frontal area
A_{acc}	amplitude of metabolic rate from metabolites (Paper III)
A_f	fundamental work constant (Paper III)
A_L	bottom area of lactic system analogy (Paper II)
A_{red}	muscle lactate recovery amplitude (Paper III)
A_{ve}	amplitude of metabolic rate from ventilation (Paper III)
a	athlete's acceleration in the course direction
B_{acc}	linear-quadratic distribution factor (Paper III)
B_f	linear coefficient of fundamental work (Paper III)
B_{ve}	linear-quadratic distribution factor (Paper III)
C_D	drag coefficient
C_DA	drag area
$E_{al,max}$	alactic system capacity (Paper III)
$E_{an,acc}$	accumulated anaerobic energy expenditure (Paper II)
$E_{an,end}$	end of race accumulated anaerobic energy (Paper II)
F_D	drag force
F_N	normal force
F_P	athlete propulsive force
F_g	gravity force
F_μ	frictional force
f	sigmoid function for smooth transition (Paper I)
GE	gross efficiency
g	acceleration of gravity
K	lactic system dampening factor (Paper III)
MAPE	mean absolute percentage error
ML	maximum lactic metabolic rate parameter (Paper II)

MR_{acc}	metabolic demand from metabolites (Paper III)
MR_{ae}	aerobic metabolic rate
MR_{al}	alactic metabolic rate (Paper III)
$MR_{ae,max}$	maximum aerobic metabolic rate
$MR_{ae,peak}$	peak aerobic metabolic rate
MR_{an}	anaerobic metabolic rate
MR_{dem}	total metabolic demand (Paper III)
MR_{f}	fundamental metabolic demand rate (Paper III)
MR_{la}	lactic metabolic rate (Paper III)
MR_{rest}	rest metabolic demand and aerobic supply (Paper III)
MR_{sub}	submaximal metabolic rate (Paper II)
MR_{sup}	metabolic supply rate (Paper III)
MR_{tot}	total metabolic demand (Paper II)
MR_{ve}	metabolic demand rate due to ventilation (Paper III)
MSE	mean square error
m	athlete body mass (may include equipment mass)
$[mLa^-]$	artificial muscle lactate concentration (Paper III)
P	athlete's propulsive power (Paper II)
P	athlete's submaximal propulsive power (Paper II)
P2	intermittent protocol of test day 2 (Paper III)
P2	intermittent protocol of test day 3 (Paper III)
PP	athlete's propulsive power output
RER	respiratory exchange ratio (the same as RQ)
RMSE	root mean square error
RQ	respiratory quotient (the same as RER)
r	course curvature radius
SPM	statistical parametric mapping
STT	sprint time trial
s	local slope direction coordinate
TE	typical error

t	time
$u1$	ergometer power output (Paper III)
$u2$	minute ventilation (Paper III)
$\dot{V}_{E,max}$	maximum minute ventilation
$\dot{V}O_2$	oxygen uptake
$\dot{V}O_{2,max}$	maximum oxygen uptake
$\dot{V}O_{2,peak}$	peak oxygen uptake
V_m	maximum muscle lactate store capacity (Paper III)
v	athlete's ground speed in the course direction
w	environmental wind speed
x	global horizontal coordinate
$\dot{x}_1$	alactic metabolic rate (Paper III)
x_2	lactic metabolic rate (Paper III)
x_3	aerobic metabolic rate primary component (Paper III)
x_4	artificial muscle lactate concentration (Paper III)
x_L	lactic system "fluid" level (Paper II)
x_P	alactic system "fluid" level (Paper II)
y	global vertical coordinate
Z_{dem}	muscle lactate recovery factor (Paper III)
α	course inclination angle
β	environmental wind angle
η_{al}	alactic recovery efficiency (Paper III)
θ	lactic system dynamic response parameter (Paper II)
λ	lactic system dynamic response parameter (Paper II)
μ	friction coefficient
ϱ	air density
τ_{ae}	time constant of the aerobic system (Paper III)
τ_{la}	time constant of the lactic system (Paper III)
ψ	aerobic system dynamic response parameter (Paper II)

1 Introduction

In endurance sports like cross-country skiing, running, and cycling, the goal when competing is to complete races in a shorter time than your opponents. To achieve this, athletes continuously try to improve their physical ability, technique, tactics, and choice of equipment. For many decades, researchers have provided more and more knowledge about, e.g., different types of training, equipment, and pacing strategies and their effect on performance. One of the foundations of this type of research is to conduct repeated testing, while altering one independent variable at a time to investigate its effect on performance. However, when it comes to endurance sports, repeated testing under race-like conditions is complicated. The race durations are usually longer than 30 minutes and due to physical exhaustion, the athletes usually require several hours of subsequent recovery before they can compete again. This makes it difficult to maintain identical conditions for all parameters beyond the investigated independent variable. One possible solution to this is to use numerical simulation, whereby a system of equations describing an athlete's power output and the specific power demands of a sport are solved numerically by a computer. Using such a setup, a numerical representation of an athlete can complete a specific race over and over with only one specific independent variable being altered at a time to study its influence on the finish time (or another metric of performance).

The use of numerical simulation for various purposes in endurance sports research has over recent decades. Early simpler examples include investigations of pacing strategies in cycling (Swain, 1997; Atkinson et al., 2007). More recent studies have been conducted to calculate of the influence of wind and friction on race times in cross-country skiing (Carlsson et al., 2011) and to optimize pacing strategies

for cross-country skiers (Sundström et al., 2013) as well as cyclists operating individually (Sundström and Bäckström, 2017), and in pairs (Wolf and Saupe, 2017). The earlier examples apply formulations of the athletes' propulsive power contributions that are empirically derived. In contrast, the latter examples use bioenergetic models that describe the athlete's bioenergetic system as a restriction in numerical simulations. The former is characterized by its simplicity and general approach, while the latter provide a more detailed representation of events and open the possibility of individualized approaches.

2 Objectives

The overall objective of this thesis was to evaluate and improve the existing state-of-the-art numerical simulation methods for endurance sports. To specify the overall objectives, the following aims were stated:

- AIM1: Evaluate the applicability of numerical modeling with propulsive power models.
- AIM2: Evaluate the validity of existing bioenergetic models.
- AIM3: Develop a bioenergetic model with improved validity and applicability regarding both describing and predicting the human bioenergetic system.

To meet these aims, the following concretized research questions were formulated and addressed in this thesis:

- RQ1: What is the impact of dynamic friction on race times in cross-country skiing? (Paper I)
- RQ2: How can bioenergetic models be adapted to reflect the bioenergetic system of a specific athlete? (Paper II and III)
- RQ3: What is the minimum error between measured and modeled aerobic metabolic rate that can be obtained using existing bioenergetic models? (Paper II)
- RQ4: How can a new bioenergetic model be formulated to
    - Reduce the error between measured and modeled aerobic metabolic rate? (Paper III)
    - Describe the behavior of the human bioenergetic system in a physiologically plausible manner? (Paper III)

2.1 Structure

The content and structure of this thesis follows the chronological order of the papers it is based on, but this order also provides a natural

progression in complexity. Chapter 3 describes the basic premises for numerical simulation, while Chapter 4 introduces a more general treatment of an athlete's power output. Paper I exemplifies the knowledge that can be gained from this approach (Section 4.2). Chapter 5 introduces a more complex approach to athletes power output using bioenergetic modeling and lead into Paper II, which evaluates the validity of two existing bioenergetic models (Section 5.3) and the subsequent development and validation of a new bioenergetic model, described in Paper III (Section 5.4).

3 Endurance sports athlete as a mechanical system

In endurance sports, an athlete in motion can be viewed as the object of study in a mechanical system. Acting upon the athlete are several forces: the mechanical resistances against the athlete and the propulsive force provided by the athlete to overcome this resistance (Figure 1). The athlete is often simplified as a point mass, since it is the overall translation of an athlete over a racecourse that is the subject of study. As such, the influence of the movements of individual body parts (e.g. arms, legs) is generally incorporated into the description of the propulsive force. The resistant forces typically included are those related to gravity, frictional resistance, and air drag.

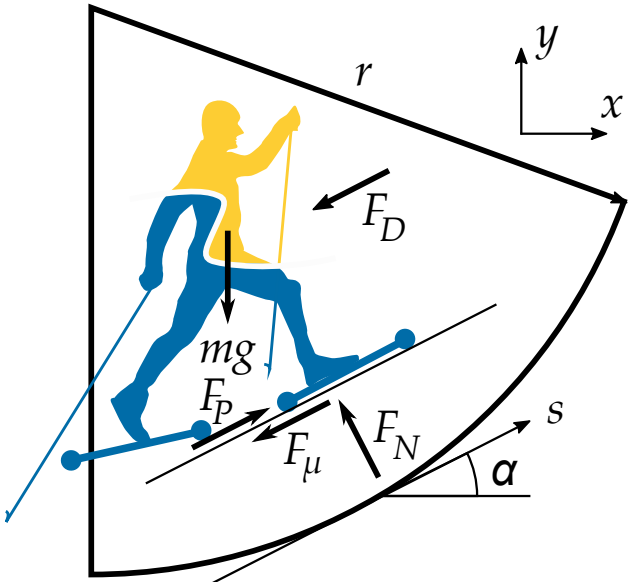

Figure 1. Free body diagram of a roller skiing athlete on arbitrary course section with resistive and propulsive forces. F_D is drag force, F_N is normal force, F_P is propulsive force, F_μ is frictional force, mg is the weight of the skier with equipment, r is course curvature radius, s is the slope direction and α is the slope inclination angle.

When moving over a racecourse of varying terrain, an athlete needs to overcome gravity when moving uphill, but will be propelled by gravity when moving downhill. Considering the athlete as a point mass on an arbitrary section of the course with an angle α between the racecourse and the horizontal line, the gravitational force F_g can be expressed as

$$F_g = mg \sin \alpha \tag{1}$$

where m is the total mass of the athlete with equipment and g is the gravitational constant. A positive or negative α indicates if the force is resisting or propelling the athlete. The frictional force F_μ will be dependent on the normal force and can be expressed as

$$F_\mu = \mu m \left(g \cos \alpha + \frac{v^2}{r} \right) \tag{2}$$

where μ is the coefficient of dynamic friction, v is the speed of the athlete's center of mass, and r is the vertical plane curvature radius of the center of mass. μ is generally related to glide friction between two surfaces, such as skis moving on snow. In the case of roller skiing or cycling, μ is replaced by the coefficient of rolling resistance C_{rr}, but equation (2) still holds. The centripetal force $\left(\frac{mv^2}{r}\right)$ is only relevant during high velocities and for small radii, and hence is sometimes omitted. The drag force F_D (from air resistance) can be expressed as

$$F_D = \frac{1}{2} \rho C_D A (v + w \cos \beta)^2 \tag{3}$$

where ρ is the density of the air, the drag coefficient C_D is a shape factor and A is the frontal projected area of the athlete and equipment, w is the external wind speed, and β is the angle between the external wind and pure head wind. Sometimes $C_D A$ is collectively referred to as

the drag area, which varies depending on speed and technique, especially in cross-country skiing. The added effect of external wind holds for pure head or tail winds ($\cos\beta = 0$). For better accuracy in the case of an external side wind, equation (3) should be adjusted to account for the resulting wind and would require a drag area additionally dependent on external wind speed and direction. However, if information about the drag area is unavailable, equation (3) still represents a reasonable approximation.

Applying Newton's second law of motion, the acceleration of an athlete, and hence her movement over a racecourse, can now be formulated as

$$ma = \frac{P_P}{v} - mg\sin\alpha - \mu m\left(g\cos\alpha + \frac{v^2}{r}\right) - \frac{1}{2}\rho C_D A(v + w\cos\beta)^2 \qquad (4)$$

where a is the acceleration along the slope tangent and P_P is the athlete's propulsive power. Equation (4) is referred to as the motion equation.

3.1 Implementation of the force balance model

When solving the motion equation (equation (4)) numerically, the racecourse is often simplified to an elevation profile. The effects of turning left or right are either treated separately or ignored. The elevation profile is often given as a set of coordinates within a global coordinate system where x is the horizontal distance and y the vertical distance. To be able to calculate derivatives of y with respect to x, the elevation curve can be expressed as a continuous chain of piecewise cubical splines. From such an elevation profile, the inclination angle α and the curvature radius r can be calculated as

$$\alpha = \tan^{-1}\frac{dy}{dx}$$
$$r = \frac{\left[1 + \left(\frac{dy}{dx}\right)^2\right]^{\frac{3}{2}}}{\left|\frac{d^2y}{dx^2}\right|} \tag{5}$$

To be able to apply the geometrical components α and r more easily, it is convenient to convert the local coordinates (slope tangent and slope normal) in equation (4) into the global coordinates x and y. This is done using the equations

$$a = \frac{d^2x}{dt^2}/\cos\alpha$$
$$v = \frac{dx}{dt}/\cos\alpha \tag{6}$$

where $\frac{dx}{dt}$ is the horizontal velocity, and $\frac{d^2x}{dt^2}$ is the horizontal acceleration.

Additionally, endurance competitions usually require athletes to cover a specific distance in as short a time as possible. Therefore, it is logical to invert equation (4) to make it distance rather than time dependent. This is done using the following equations

$$\frac{dx}{dt} = \left(\frac{dt}{dx}\right)^{-1}$$
$$\frac{d^2x}{dt^2} = -\frac{d^2t}{dx^2}\left(\frac{dt}{dx}\right)^{-3} \tag{7}$$

Combining equation (4), (6), and (7) gives

$$\frac{d^2t}{dx^2} = -\left(\frac{dt}{dx}\right)^4 \frac{P_P}{m}\cos^2\alpha + g\sin\alpha\cos\alpha\left(\frac{dt}{dx}\right)^3 +$$
$$\mu\left(g\cos^2\alpha\left(\frac{dt}{dx}\right)^3 + \frac{1}{r\cos\alpha}\frac{dt}{dx}\right) + \frac{1}{2}\frac{\rho C_D A}{m\cos\alpha}\left(\frac{dt}{dx}\right)^3\left(\left(\frac{dt}{dx}\right)^{-1} + w\cos\beta\right) \tag{8}$$

Using variable substitution, equation (8) can be split into a system of two first order differential equation and solved with standard ordinary differential equation solvers in e.g. MATLAB, if a function of the propulsive power is provided. While the resistant forces in equation (4) depends mostly on external parameters, such as the slope of the racecourse and interactions between equipment and the environment, propulsive power (and to some extent the drag area) depends on the specific sport and the athlete's technical and physiological capabilities.

4 The human body as a machine

When an endurance sport athlete is described as a mechanical system, the human body can be viewed as a machine or propulsive engine. Simply by making this analogy we tend to neglect the psychological aspects of endurance performance. While the human body is not a machine, the analogy is nevertheless instructive when it comes to providing knowledge about the propulsive power needed for numerical simulations. Attempts to describe the human body as a machine have been made with various levels of sophistication, from the use of constant or linear power output to elaborate attempts at mimicking the metabolic energy supply systems of humans.

4.1 Propulsive power models

Many research studies have used a propulsive power model based on empirical data (Swain, 1997; Atkinson et al., 2007), the researchers knowledge of the specific sport (Carlsson et al., 2011; Sundström et al., 2013), or a combination thereof (Moxnes et al., 2014). The simplest of these models are based on constant propulsive power from the athlete, while more advanced are based on sigmoid functions that result in a near constant propulsive power at low velocities that decrease increasingly quickly as the athlete approaches a critical velocity and eventually reach zero propulsion. Maybe the most advanced and rigorously developed model of propulsive power for cross-country skate skiing to date comes from Gløersen et al. (2018). It combines previous research with field measurements and numerical simulations to establish a model for propulsive power dependent on velocity, acceleration, and body mass given by

$$P_P = (7.26 - 0.54v - 0.71a) \cdot m \tag{9}$$

It also includes a model of drag area as a function of velocity, body mass, air density and air viscosity (see Gløersen et al. (2018)). The model was derived from measurements with eight high-level male cross-country skiers individually skiing 13.5 km under race like conditions. Hence, the model is assumed valid only under circumstances similar to those.

4.2 Influence of dynamic friction on performance in cross-country skiing

In Paper I, equation (8), with the addition of equations for propulsive power and drag area according to Gløersen et al. (2018), was solved in MATLAB (R2020b, Mathworks Inc., Natick, MA, United States) to investigate the influence of the dynamic friction coefficient on race times in cross-country skiing. Five values of frictional coefficient (μ = 0.005, 0.013, 0.015, 0.025, 0.027), three values of body mass (m = 70, 80, 90 kg), and three wind speeds (w = 4 NE, 0, 4 SW) $m \cdot s^{-1}$ were used. Equation **Error! Reference source not found.** was solved for all c ombinations of the parameter values (n = 45) for both a 15.6 km racecourse (5 laps of the 3 km biathlon racecourse at the Östersund biathlon stadium; Figure 2) and an artificial racecourse consisting of

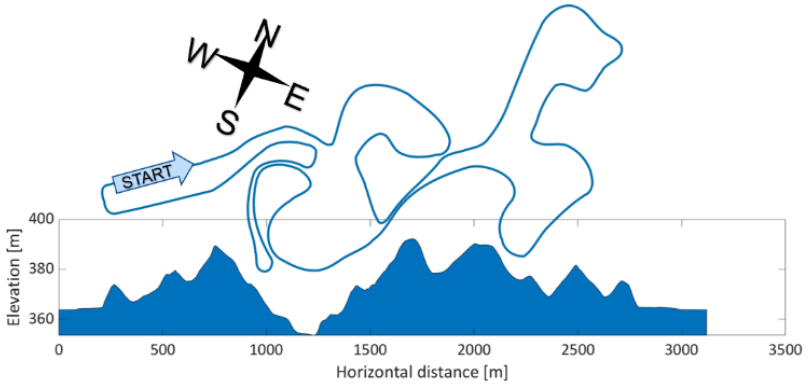

Figure 2. Map overview and elevation profile of the 3 km racecourse at Östersund Biathlon Arena

long sections at specific angles of incline (α = -7°, -3.5°, 0°, 3.5°, and 7°). The propulsive power model was slightly modified to give a somewhat smoother transition to zero at higher speeds by multiplying equation (9) with the sigmoid function

$$f = \frac{1}{1 + e^{(3(v-9.1))}} \tag{10}$$

To assess the legitimacy of the propulsive power model, a comparison was made between average propulsive power calculated according to Gløersen et al. (2018) and body mass scaling (Bergh, 1987) using the average power of the 80 kg skier calculated according to Gløersen et al. (2018) as a baseline (Table 1). The difference in average propulsive power per body mass is greater when calculated according to Gløersen et al. (2018), but the difference in average propulsive power is less than 3% for each of the skiers between the two methods of calculation.

Table 1. Comparison of average propulsive power from the 15.6 km race with μ = 0.015 and no external wind for three simulated skiers of different body masses. The average propulsive power is calculated according to Gløersen et al. (2018) and body mass scaling (Bergh, 1987) using the average power of the 80 kg skier calculated according to Gløersen et al. (2018) as a baseline.

Average propulsive power	**70 kg**	**80 kg**	**90 kg**
Gløersen et al. (2018) [W]	187.8	210.9	233.0
Bergh (1987) [W]	193.0	210.9	228.2

The isolated influence of dynamic friction on average pace during the 15.6 km race is shown in Figure 3. As an example, increasing μ from 0.013 to 0.015 for any of the three skiers resulted in a 34-second increase in finish time. This change is comparable to the effect different ski preparations (Budde and Himes, 2017), and is more than enough to be a determining factor in a close race. A change of μ from 0.005 to 0.027

(e.g. from a sudden snow fall) increased the finish time by more than 6 minutes.

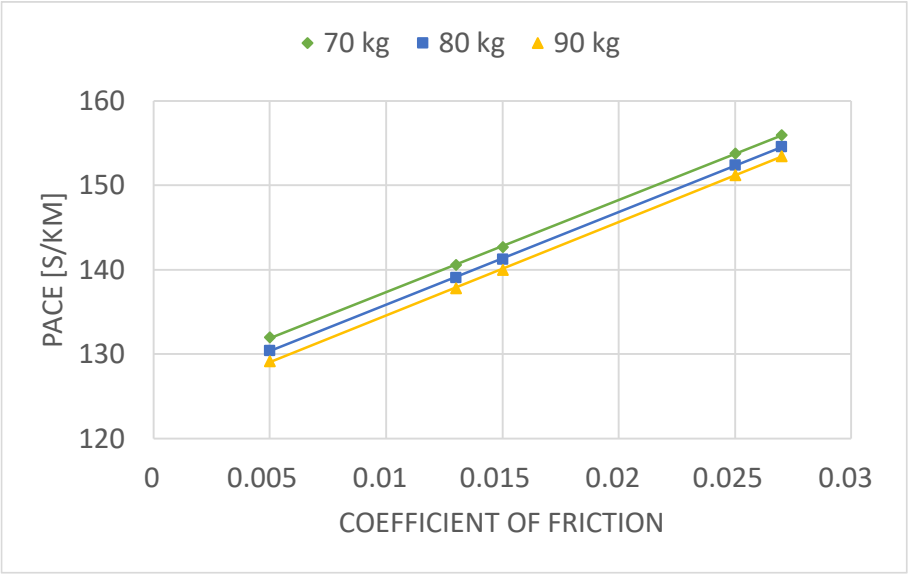

Figure 3. Influence from coefficient of friction on average pace for the entire 15.6 km race for the 70 kg, 80 kg and 90 kg skier, respectively

From the artificial racecourse, it was concluded that a change in speed occurring when increasing μ from 0.013 to 0.015 would be most significant for moderate downhill terrain, followed by flat and moderate uphill terrain. However, since more time is spent moving uphill (due to the lower speeds on this terrain), changes in race times are mostly affected by uphill sections, as can be seen in Figure 4. For instance, when increasing μ from 0.013 to 0.015 for an 80 kg skier, 70% of the difference in race time originated from the uphill sections. In this

case, flat was defined as an incline of $-1° \leq \alpha \leq 1°$ and 37% of the race distance was uphill.

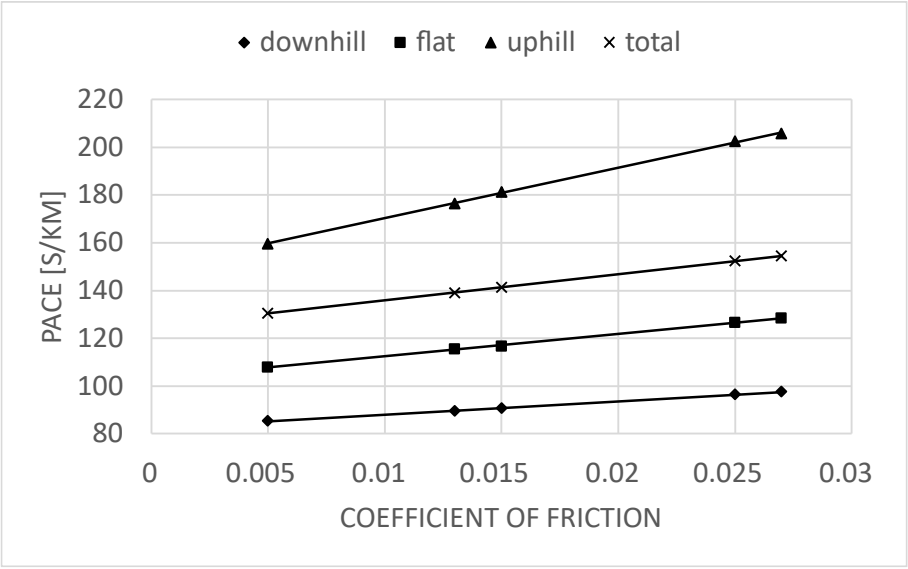

Figure 4. Influence from coefficient of friction on average pace in downhill, flat, uphill or total, respectively

4.3 Limitations of propulsive power model and group mean values

Paper I provides an example of the kind of knowledge that can be gained with the aid of numerical simulation of endurance sports. For such purposes, propulsive power models work well. However, propulsive power models to date have been based on group mean data with individual adaptations based only on body mass. Fatigue effects are averaged into the propulsive power models and any individualizations beyond the group mean dependency on body mass is neglected. For equipment-to-environment or some athlete-to-environment effects where the group average approach is of interest, the propulsive power models may suffice. But race tactics and training

programs need to be individually adapted, since every athlete has their own individual prerequisites. Although both individual adaptations and fatigue effects could be incorporated into a propulsive power model, they have so far been addressed by modeling the human metabolic energy supply systems with bioenergetic models.

5 Beyond machine – the human metabolic energy system

Skeletal muscle contraction is powered by the release of energy through the breakdown of adenosine triphosphate (ATP). Since only a small amount of ATP is available in human skeletal muscles, it has to be replenished to maintain sufficient availability, which occurs cia three separate systems. The alactic system can deliver a small amount of ATP at a high rate through the breakdown of phosphocreatine (PCr), which is available in human skeletal muscles. A significantly larger amount of ATP can be delivered by the lactic system through the breakdown of glucose molecules from stored glycogen (glycolysis), but at a much lower rate. Finally, ATP concentration can be maintained for several hours of exercise by the aerobic system through mitochondrial respiration, but at an even lower rate. In this process pyruvate, derived from glycolysis and fatty acids, is oxidized, which leads to a large amount of energy being released that can be used to generate ATP. The rate of the aerobic system is limited by the availability of oxygen to the mitochondria (McArdle et al., 2009).

The metabolic rate of the aerobic system can be measured through indirect calorimetry, however, the remaining two energy systems (together referred to as the anaerobic system) are not easily measured. Although the aerobic system is the major determinant of performance in endurance sports, the anaerobic system is also important in disciplines characterized by varying intensity, such as cycling and cross-country skiing (Skiba et al., 2012; Gløersen et al., 2020). Over varying terrain, the anaerobic system is utilized during periods of greater exertion, such as uphill sections of a course, where the aerobic system cannot meet the metabolic demand, resulting in oxygen deficits that are repaid during periods of lower exertion (Gløersen et al., 2020). This

discharge-recharge of the anaerobic stores occurs across different time intervals and exercise intensities throughout the full duration of sports activities. Since only the aerobic metabolic rate can be easily measured, a bioenergetic model is needed to relate the expenditure level of the anaerobic stores to the aerobic metabolic rate and power output.

5.1 Bioenergetic modeling

The field of human bioenergetic modeling starts with the introduction of the critical power concept for local muscle work capacity by Monod and Scherrer (1965), which was later extended to full body work by (Moritani et al., 1981). The critical power concept simplifies the human bioenergetic system into two components: a finite aerobic metabolic rate (referred to as the critical power) and a finite anaerobic work capacity. The power demand of working muscles is supplied by the aerobic system up to the critical power threshold. Exceeding the critical power threshold, the excess power demand will be met by the anaerobic work capacity until depleted, at which time power output is limited to critical power. Despite the drawback of an instant and infinite power supply at the critical power level, several variations of the critical power model have been proposed, including several that go beyond the assumptions of the critical power concept. Only bioenergetic models that incorporate anaerobic recovery are relevant for this thesis, and as such any models that do not fulfil this criterion have not been considered.

(Morton and Billat, 2004) developed a model based on the critical power concept that can be applied to intermittent exercise, in which a finite energy store (comparable to anaerobic capacity) can be utilized and recovered, with the utilization and recovery rates dependent on metabolic demand. Skiba et al. (2012, 2015) further developed the

model by introducing a curvilinear recovery of the finite energy stores in line with the findings of (Ferguson et al., 2010). The simple formulations of these models make them easily applicable, but they do not take any variation of the aerobic metabolic rate into account.

Another model of metabolic energy supplied from either the aerobic or anaerobic system was described graphically by Morton (2006). As this model includes variations in the power supplied by the aerobic system it cannot be considered a critical power model. This model is a simplified version of the Margaria-Morton model, proposed as an idea by Margaria (1976), in which all three metabolic energy supply systems are modeled. Morton (1986, 1990) mathematically described this approach and derived restrictions based on empirical data, however, neither of the models was fully validated. The Margaria-Morton model was further developed into the Margaria-Morton-Sundström model by Sundström (2016) to e.g., differentiate between carbohydrate and fat utilization, but neither this model was fully validated.

Two models suggested by Stirling et al. (2005) and Artiga Gonzalez et al. (2019) respectively, attempt to model the dynamics of the aerobic metabolic system in a manner similar to the widely accepted description of the aerobic system as the sum of a constant baseline and three exponential functions with their own separate error signals, time constants, and time delays (Poole and Jones, 2012). The first exponential function (the cardio dynamic component) has a small magnitude and duration and is therefore often incorporated into the second exponential function (the primary component). For the third exponential function (the slow component), several underlying, and possibly overlapping, mechanisms have been suggested, e.g., a drift in metabolic demand, reduced efficiency in recruited muscle fibers, and successive recruitment of less efficient muscle fibers (Poole and Jones,

2012). The model by Artiga Gonzalez et al. (2019) was validated for 5 cyclists over 4 different protocols and showed good agreement with measurements. However, the model offers no information on variations in the anaerobic systems. The model by Stirling et al. (2005) offers a methodology for determining the actual metabolic demand and predicting the contribution of the aerobic system, which in turn makes it possible to calculate the contribution of the anaerobic system. However, when (Moxnes et al., 2014) tested the model at four different constant power levels with subsequent recovery, it yielded poor results at higher intensities. The study also tested three additional models for the aerobic system, the last of which used the power contribution from the lactic system, approximated from measured blood lactate, as an input. This last model showed good agreement with measured aerobic metabolic power, despite not capturing the exact dynamics. However, estimating lactic power from measurements of blood lactate is a crude approach, and since this is used as an input, the model offers poor additional information on the dynamics of the lactic system.

In summary, there is a plethora of proposed bioenergetic models, but only a few describe the dynamics of all three metabolic energy systems, most lack thorough validation and few attempts have been made of individualization. To obtain reliable and relevant data, these shortcomings need to be addressed.

5.2 Individual adaptations of bioenergetic models

The bioenergetic models proposed (Section 5.1) are based on knowledge of the dynamics of the human metabolic energy systems and provide a general picture applicable at a group level. However,

we also know from experience that humans vary substantially from one another. This is true even in elite cross-country skiing where the body mass of athletes in the same race could differ by 20 kg, and athletes with large anaerobic capacities compete against those with relatively small anaerobic capacities but extremely efficient aerobic systems. Thus, to fully utilize a bioenergetic model, the general formulation needs to be adapted to a specific athlete to provide relevant knowledge for decision making about training programs or race tactics. With the basic bioenergetic model formulation given, individualizing the model requires optimizing certain parameters such that the dependent variables of the model best reflect the behavior of each athlete's bioenergetic system. In the case of a non-linear model (e.g., including differential equations), this process is referred to as non-linear grey-box parameter estimation.

The bioenergetic models are formulated to accept one or several time series of measured data as an input (independent variables) and return one or more times series of output data (dependent variables). The formulations may also include mediating variables calculated as steps towards obtaining the dependent variables and, most importantly, will include parameters. These parameters may be constants, e.g., the gravitational coefficient g, which is unlikely to change, or individual parameters, e.g., maximum oxygen uptake ($\dot{V}O_{2,max}$), which needs to be adjusted to match each athlete.

The parameter estimation process uses the independent variable data to solve the bioenergetic model equations for a specific set of parameter values, calculate the remaining error (e.g., the mean square error; MSE) between the calculated and measured dependent variable, and then adjust the parameter values using a search algorithm to try to further reduce the remaining error. The process is repeated until it converges,

i.e., either the reduction of the remaining error or the adjustment of the parameters is smaller than a specified limit value, at which point an optimal set of parameters is considered to have been found. To avoid unrealistic parameter values, restrictions on the range of each parameter must often be implemented. The search algorithm may also converge towards a local optimum, so an additional global optimization method needs to be used to increase the probability of the true global optimum being found.

There are examples of individual adaptations performed by setting selected parameters to known individual values from experimental testing (Sundström, 2016; Wolf and Saupe, 2017), but the only found record of the parameters of a bioenergetic model being optimized according to the parameter estimation process described above is in research by Artiga Gonzalez et al. (2019).

5.3 Validation of two bioenergetic models

Of the highlighted models, only the Margaria-Morton model and the Margaria-Morton-Sundström model provide relationships that can be used to predict the contributions of the aerobic, lactic, and alactic systems, although have not been fully validated. The aim of Paper II was to develop a method of individual adaptation applicable to the Margaria-Morton model (Figure 5A) and the model by Morton (2006) (Figure 5B), as well as validate their ability to replicate the behavior of the human bioenergetic system on an individual basis. The Margaria-Morton-Sundström model was excluded due to its complexity.

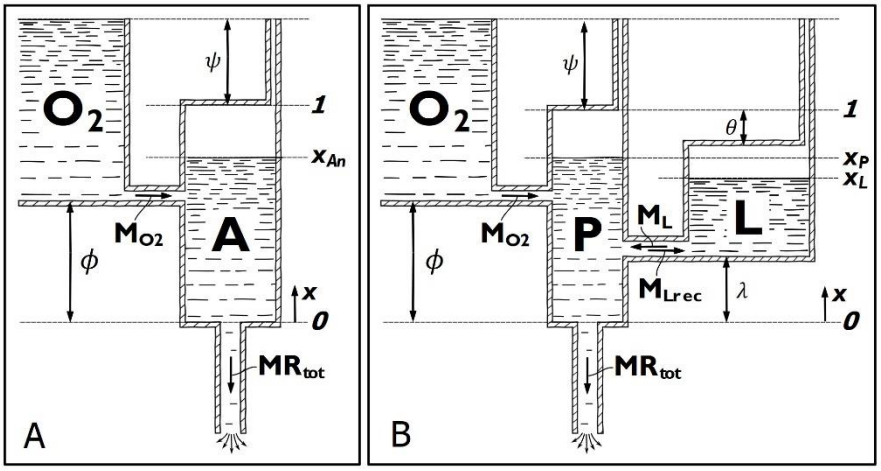

Figure 5. Diagrammatical representations of the critical-power derived two-tank model (2TM) (Panel A) and the adjusted Margaria-Morton three-tank model (3TM) (Panel B).

5.3.1 Study design

In the models in Paper II, the available energy from the modeled energy supply systems is depicted as fluid in a tank and the utilization of energy as fluid flow from each of the tanks (Figure 5). The relative size and positioning of the tanks and the flow capacity of their interconnecting pipes define the dynamic behavior of the system. For instance, the power output from the lactic system is governed by the difference in "fluid" level between the lactic system (x_L) and the alactic system (x_P) in relation to the maximum possible difference ($1 - \theta - \lambda$) multiplied by the maximum possible flow (M_L) through the pipe connecting the lactic system (L-tank in Figure 5B) and the alactic system (P-tank) according to

$$A_L \frac{dx_L}{dt} = -\frac{x_L - x_P}{1 - \theta - \lambda} M_L \tag{11}$$

where A_L is the bottom area of the L-tank and $\frac{dx_L}{dt}$ is the rate of change of the fluid surface level in the L-tank. Hence, $A_L \frac{dx_L}{dt}$ is the power

output from the lactic system. In this example, A_L, M_L, θ, and λ are parameters included in the parameter estimation for the individualization of the model.

Both models in Paper II are slightly modified from their original descriptions, with the introduction of the parameter ψ, which allows the O_2-tank to extend beyond x = 1 as originally suggested by Sundström (2016). This introduces a base-level aerobic power output that is available before the other metabolic systems are utilized (comparable to aerobic power at rest). To differentiate the models in Paper II from those originally proposed, they are referred to as 2TM (Figure 5A) and 3TM (Figure 5B). Two variations of each model were validated with the M_{O2} parameter either included in the parameter estimations (2TM-free and 3TM-free, respectively) or fixed to each subjects peak aerobic power ($MR_{ae,peak}$) from measurements (2TM-fixed and 3TM-fixed, respectively).

Experimental data were taken from a previous study, in which eleven male cross-country skiers (age: 24.3 ± 3.6 years, height: 182.1 ± 5.1 cm, body mass: 78.7 ± 5.9 kg, equipment mass: 4 ± 0.1 kg, $\dot{V}O_{2,max}$ 67.5 ± 3.2 mL·kg^{-1}·min^{-1}), competing at a national or international level, performed submaximal exercise tests for the assessment of gross efficiency and four self-paced roller-skiing sprint time trials (STT) over undulating terrain on a motor-driven treadmill (Rodby Innovation AB, Vänge, Sweden; Andersson et al., 2017). Pulmonary oxygen uptake ($\dot{V}O_2$) was monitored continuously using an ergo-spirometry system AMIS 2001 (Innovision A/S, Odense, Denmark). The main performance test consisted of four STTs interspersed with 45 minutes of recovery. However, in Paper II, only physiological and kinematic data from the first sprint time trial (STT1) and second sprint time trial (STT2) were analyzed. The course profile consisted of three flat

sections (1°) interspersed with two uphill sections (7°). The participants used double poling on the flat sections and diagonal stride on the uphill sections (see course profile in Figures 6 and 7). The distance traveled was recorded every 0.406 s, resulting in $n = 527$ to 601 synced values for, time, speed, and position, along the course, as well as STT finish time.

Total metabolic rate in Watts was calculated according to the following power balance model

$$MR_{tot} = \frac{P}{GE} = \frac{mgv(\sin\alpha + \mu\cos\alpha)}{GE} \tag{12}$$

where P is the power output and GE is gross efficiency. Individual gross efficiency relationships were derived by combining steady-state power output and regression analysis of submaximal metabolic rates as functions of speed and slope, according to

$$GE = \frac{P_{sub}}{MR_{sub}} \tag{13}$$

where P_{sub} is the estimated power output in the submaximal tests and MR_{sub} is the corresponding metabolic rate calculated as

$$MR_{sub} = \dot{V}O_2(76.7RER + 272) \tag{14}$$

where RER is the measured respiratory exchange ratio. The aerobic power from measurements (MR_{ae}) was also calculated according to equation (14) but with RER set to 1.0 (i.e. assuming 100% carbohydrate utilization). The anaerobic power was calculated as

$$MR_{an} = MR_{tot} - MR_{ae} \tag{15}$$

For further details about the experimental setup, see Paper II.

The parameter estimation, as described in Section 5.2, was implemented to work for the 2TM and 3TM models. The models included MR_{ae} and MR_{an} as dependent variables (MR_{an} being the sum of lactic and alactic power for 3TM), so for the parameter estimation, the weighted sum of the MSE of both variables was used as a cost function (function to be minimized). The MSE of MR_{ae} was assigned a weight 1, while the weight of MSE of $E_{an,acc}$ for each subject was calculated as

$$weight = \left(\frac{\overline{MR}_{ae}}{\bar{E}_{an,acc}}\right)^2 \tag{16}$$

where $\overline{MR}_{ae}$ and $\bar{E}_{an,acc}$ are the measured mean in STT1 of the aerobic metabolic rate and accumulated anaerobic energy expenditure, respectively. To ensure a global optimum, a multi-start method was applied, such that the parameter estimation for each subject and model was run with various combinations of initial parameter values. This gave a total of 144 combinations of initial parameter values to be run for each subject for 3TMs and a total of 18 combinations for each subject for 2TMs.

The root mean squared errors (RMSE) of aerobic metabolic rate (MR_{ae}) and accumulated anaerobic energy expenditure ($E_{an,acc}$) were used to evaluate the model validity, both in absolute terms and as percentage of the STT mean values.

5.3.2 Results

The model-to-measurement mean difference and typical errors in both MR_{ae} and $E_{an,end}$ were small for STT1 but noticeably larger for STT2 (see Figure 4 and 5 in Paper II). Moreover, the model-to-measurement mean difference typical error was lower for 2TM-free compared to the other models in both MR_{ae} and $E_{an,acc}$ for STT1 and STT2.

The median RMSE of both MR_{ae} and $E_{an,acc}$ were significantly lower for 2TM-free compared to the other three models in STT1 (Table 2). Nonetheless, the RMSE for all models were relatively small in STT1, indicating the suitability of the implemented parameter estimation method. The results from STT1 also show the greatest potential of the models.

Table 2. The median of the root mean square errors for the aerobic metabolic rate and accumulated anaerobic energy expenditure as a percentage of the respective means for STT1 and STT2. This is a selection of data from Table 2 in Paper II.

		2TM-free	2TM-fixed	3TM-free	3TM-fixed
STT1	MR_{ae}	3.4%	5.7%	5.3%	6.1%
	$E_{an,acc}$	1.3%	3.8%	1.8%	2.6%
STT2	MR_{ae}	5.1%	5.8%	6.5%	7.5%
	$E_{an,acc}$	11.7%	14.1%	14.4%	17.2%

The median RMSE were larger In STT2 overall, but the 2TM-fixed resulted in an almost equal RMSE of MR_{ae} in both STTs, indicating that it might be the most reliable model of the four. The large RMSE of $E_{an,acc}$ may mainly be explained by the differences in the subjects' performance between STT1, for which the mean value of $E_{an,end}$ was 70.4 kJ and STT1, for which the equivalent value was 47.9 kJ. The same values for MR_{ae} were 1.54 kW and 1.56 kW, respectively.

Comparisons of MR_{ae} and $E_{an,end}$ for each respective bioenergetic model versus the measurement data are shown as group mean time series for STT1 and STT2 in Figure 6 and Figure 7, respectively. The trend for STT1 was lower RMSE for 2TM-free and 3TM-free compared to their counterparts 2TM-fixed and 3TM-fixed (Table 2). However, Figure 6 indicates that M_{O2} (i.e., $MR_{ae,max}$) in 2TM-free and 3TM-free was decreased to a value below $MR_{ae,peak}$. Here, it is advantageous to

match the almost constant MR_{ae} during the last two thirds of STT1, but the models would not be able to reflect the subjects' true $MR_{ae,max}$. In both Figure 6 and Figure 7 it is also clear that all four models capture the general pattern of both MR_{ae} and $E_{an,acc}$, but in most cases fail to capture the details.

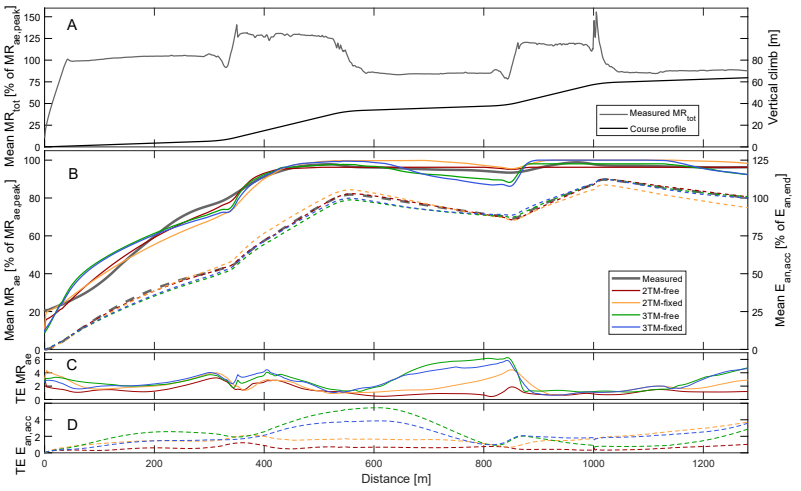

Figure 6. Measured and modeled metabolic variables during STT1 including (A) group mean of total metabolic rate (MR_{tot}), course profile, (B) mean aerobic metabolic rate (MR_{ae}, solid), accumulated anaerobic energy expenditure ($E_{an,acc}$, dashed), (C) typical error of aerobic metabolic rate (TE MR_{ae}), and (D) typical error of anaerobic accumulated energy expenditure (TE $E_{an,acc}$). Metabolic rates are expressed relative to peak aerobic metabolic rate in STT1 ($MR_{ae,peak}$) and accumulated anaerobic energy expenditure is expressed relative to the accumulated anaerobic energy expenditure at the end of the course ($E_{an,end}$).

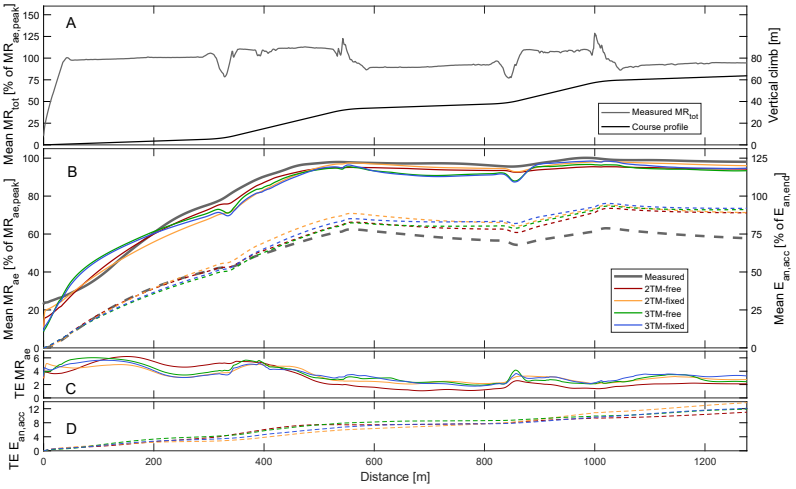

Figure 7. Measured and modeled metabolic variables during STT2 including (A) group mean of total metabolic rate (MR_{tot}), course profile, (B) mean aerobic metabolic rate (MR_{ae}, solid), accumulated anaerobic energy expenditure ($E_{an,acc}$, dashed), (C) typical error of aerobic metabolic rate (TE MR_{ae}), and (D) typical error of anaerobic accumulated energy expenditure (TE $E_{an,acc}$). Metabolic rates are expressed relative to peak aerobic metabolic rate in STT1 ($MR_{ae,peak}$) and accumulated anaerobic energy expenditure is expressed relative to the accumulated anaerobic energy expenditure at the end of the course ($E_{an,end}$).

5.3.3 Conclusions

One conclusion from Paper II was that to fully evaluate the validity of a bioenergetic model, a test protocol with more variable intensity should be used, in part to test the model at different exercise intensities and recovery, and in part to aid the parameter estimation process by including larger variations in the dependent variables.

Paper II also revealed that the Margaria-Morton model can likely not provide reliable knowledge about the human bioenergetic system, as it was outperformed by a less complex model. Since the Margaria-Morton model, apart from the much more complex Margaria-Morton-Sundström model, is the only known attempt at mathematically

describing the three major metabolic energy supply systems, a new model is needed to provide this knowledge.

5.4 Development and validation of a new bioenergetic model

Paper III details the development and validation of a new bioenergetic model that describes the contributions of the alactic, lactic, and aerobic systems as well as different sources of the total metabolic demand.

5.4.1 Metabolic supply formulation

In the developed model, the energy supply can be expressed, in terms of metabolic rate, as

$$MR_{sup} = MR_{al} + MR_{la} + MR_{ae} = \dot{x}_1 + x_2 + x_3 + MR_{rest} \tag{17}$$

Where $MR_{al} = \dot{x}_1$ is the alactic system metabolic rate, $MR_{la} = x_2$ is the lactic system metabolic rate, and

$$MR_{ae} = MR_{rest} + x_3 \tag{18}$$

is the aerobic system metabolic rate. MR_{rest} is both the metabolic demand and the aerobic metabolic supply rate at sitting rest, but does not include the metabolic demand due to ventilation, which is treated separately. x_3 is the primary (only) component of aerobic metabolic rate. The bioenergetic system metabolic rates ($\dot{x}_1, x_2, x_3$) and an artificial muscle lactate concentration ([mLa$^-$] $= x_4$) are governed by the following system of time-dependent differential equations:

$$\begin{cases} \dot{x}_1 = (MR_{dem} - MR_{rest} - x_3 - x_2)/E_{al,max} \\ \dot{x}_2 = (MR_{dem} - MR_{rest} - x_3 - x_2)/\tau_{la} - K \cdot \dot{x}_3 \\ \dot{x}_3 = (MR_{dem} - MR_{rest} - x_3)/\tau_{ae} \\ \dot{x}_4 = (x_2 - A_{red} \cdot Z_{dem} \cdot x_4)/V_m \end{cases} \tag{19}$$

The rate of change of the aerobic metabolic rate $\dot{x}_3$ is regulated with an error signal ($MR_{dem} - MR_{rest} - x_3$), and a time constant τ_{ae} controlling the response time. The error signal is the difference between the total metabolic demand (MR_{dem}) and the current aerobic metabolic rate ($MR_{rest} + x_3$). In a dynamic model formulation, this is equivalent to a mono-exponential response without time delay which, is a common simplification of the aerobic system response at the onset of moderate intensity exercise. As state earlier, one of the suggested causes of the aerobic slow component during higher intensities is a drifting demand. Therefore, we hypothesize that the suggested mono-exponential, in combination with drifting metabolic demand will capture the complete dynamic behavior of the aerobic system even at higher intensities.

The lactic system is considered the part of glycolysis causing an accumulation of lactate from pyruvate that cannot be immediately oxidized. Given the close relationship between the lactic and aerobic systems, we propose that the rate of change of the lactic system $\dot{x}_2$ is similarly regulated by an error signal ($MR_{dem} - MR_{rest} - x_3 - x_2$) and a time constant ($\tau_{la}$). Here, the error signal is the difference between the total metabolic demand and the sum of the current aerobic metabolic rate and current lactic metabolic rate. Additionally, the response of the lactic system is dampened by a factor *K* multiplied by the rate of change of the aerobic metabolic rate. This was added to avoid overshooting the lactic system, that would lead to unrealistic recovery of the alactic system during periods of exertion.

Equation (19) further dictates that the metabolic demand not met by the aerobic or lactic systems is instantaneously met by the alactic system. Should the alactic metabolic rate $\dot{x}_1$ fall below zero, only part of the energy diverted to the alactic recovery is converted into usable

alactic energy due to the inevitable hysteresis cost of recovery. This is expressed in equation (20), where η_{al} is the efficiency of alactic recovery and thus the hysteresis cost is $(1 - \eta_{al}) \cdot \dot{x}_1$.

$$\dot{x}_1 < 0 \Rightarrow \dot{x}_1 = \eta_{al} \cdot \dot{x}_1 \tag{20}$$

Finally, equation (19) describes the rate of change of [mLa^-], which increases when the lactate system is active and is reduced during periods of lower exertion. Additional equations and conditions on the supply side are given in Paper III.

5.4.2 Metabolic demand formulation

In the model, metabolic demand is comprised of several parts. The total metabolic demand is given by

$$MR_{dem} = MR_{rest} + MR_f + MR_{ve} + MR_{acc} \tag{21}$$

The fundamental metabolic demand rate (MR_f) is modeled by equation (22) as a linear function of the measured power output from the cycle ergometer u_1.

$$\begin{cases} MR_f = A_f + B_f \cdot u_1 \\ u_1 = 0 \Rightarrow MR_f = 0 \end{cases} \tag{22}$$

A_f, in theory, is the metabolic demand rate of unloaded cycling and B_f the increase in metabolic demand per unit increase in power output. Additionally, MR_f is set to 0 when the power output is 0, i.e., during passive rest. The metabolic demand due to ventilation is not included in MR_f, hence it differs from the often-used linear relationship between metabolic rate and power output that can be established at submaximal workloads.

The metabolic demand rate due to ventilation (MR_{ve}) has been shown to vary non-linearly with minute ventilation (Vella et al., 2006) and here it is assumed that a single relationship between MR_{ve} and the measured minute ventilation u_2 is valid for all measured u_2 and that in theory $u_2 = 0$ would result in $MR_{ve} = 0$. MR_{ve} is given by equation

(23), where A_{ve} is the maximum metabolic demand rate due to ventilation, $\dot{V}_{E,max}$ is the maximum measured minute ventilation, and B_{ve} is a distributing factor between a linear and a quadratic response.

$$MR_{ve} = A_{ve}\left(B_{ve}\left(\frac{u_2}{\dot{V}_{E,max}}\right) + (1 - B_{ve})\left(\frac{u_2^2}{\dot{V}_{E,max}}\right)\right) \quad (23)$$

Based on the assumption that equation (23) is valid for all measured u_2, metabolic demand due to ventilation is not included in MR_f and MR_{rest}.

Metabolic demand associated with the accumulation of metabolites in the muscles MR_{acc} is given by equation (24). Though the accumulation of lactate itself may be the cause of a rise in metabolic demand due to lactate shuttling, the [mLa^-] in this model is used as a proxy for the concentration of various accumulated metabolites that may cause additional metabolic demands (Gaesser and Brooks, 1984). The metabolic demand associated with accumulated metabolites is given the same form as the metabolic rate from ventilation.

$$MR_{acc} = A_{acc}(B_{acc} \cdot x_4 + (1 - B_{acc}) \cdot x_4^2) \quad (24)$$

A_{acc} is the maximum amplitude of metabolic demand from accumulated metabolites and B_{acc} is the distributing factor between a linear and a quadratic response.

5.4.3 Study design

Experimental data for the validation was collected from fourteen well-trained male cyclists (age: 35 ± 8 years, height: 181 ± 5 cm, weight: 74 ± 6 kg, $VO_{2,peak}$: 66.2 ± 5.8 ml·min^{-1}·kg^{-1}) performing 3 separate days of testing on a cycle ergometer. The first day of testing aimed to establish individual ergometer power output levels for the intermittent protocols of test day 2 (P2) and test day 3 (P3), which were designed to activate all three metabolic energy systems to different degrees and allow recovery in-between (Figure 8).

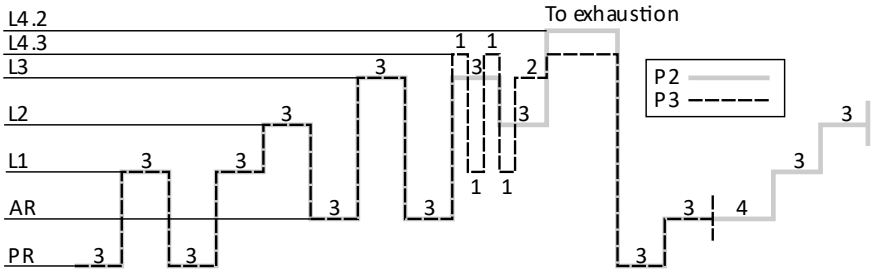

Figure 8. Intermittent test protocols used during test day 2 (P2) and test day 3 (P3). PR is passive rest, AR is active rest, and L1, L2 etcetera are individual ergometer power output levels calculated to activate the subjects' different metabolic energy systems to varying degree. Numbers show the time in minutes for each bout.

The breath-by-breath oxygen uptake ($\dot{V}O_2$) and respiratory quotient (RQ) were obtained using an automated metabolic measurement system (Moxus Modular Metabolic System; AEI Technologies Inc., Pittsburg, USA) and MR_{ae} was calculated according to (McArdle et al., 2009, Table 8.1) as

$$MR_{ae} = (1.232 \cdot RQ + 3.8149) \cdot \dot{V}O_2 \cdot \frac{4184}{60} \tag{25}$$

This was the dependent variable used for the parameter estimation and assessment of the validation. The method of parameter estimation, as described in Section 5.2, was adapted and applied to the new model with measurement data from P2 with a multi-start algorithm running 64 combinations of initial values for each subject. The same individualized models were then applied to measurement data from P3. Data from P2 are considered to show the validity and reliability of the combination of the model formulation, parameter estimation, measurement error, and data preprocessing, while data from P3 additionally includes day-to-day variation and protocol differences. As a measure of the overall model agreement with

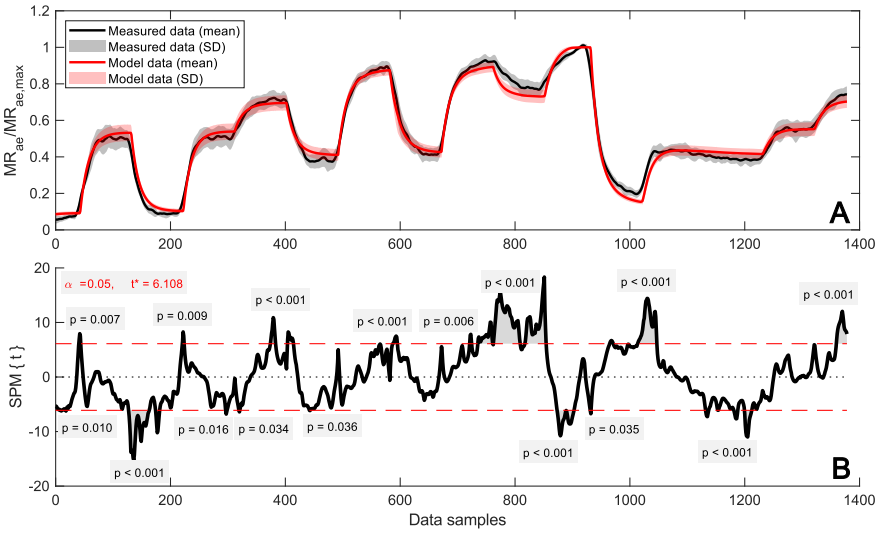

Figure 9. Time resolved mean and SD (Panel A) and statistical parametric mapping from the two-tailed paired t-test (Panel B) of measured and modeled MR_{ae} normalized with $MR_{ae,max}$ for P2 (n=11). Results from three subjects are omitted due to deviations in duration during one or more periods (same subjects as in Figure Figure 10). Data for the period leading to volitional exhaustion has been stretched/squeezed to allow averaging across the subjects. The dashed lines show the critical t-value, indicating the limit for significant differences (P < 0.05) between measured and modeled data.

measurements, the RMSE in W between measured and modeled MR_{ae} was calculated with the time-resolved data (0.5 Hz) for each subject. Using the same data, the mean absolute percentage error (MAPE) was calculated with measurement data as a base and used as an overall measure of the model's agreement with the measurements in relative terms. Statistical parametric mapping (SPM) was used to test for differences between the measurements and the model.

5.4.4 Results

For P2, the RMSE of MR_{ae} between measured and modeled data was 61.9 ± 7.9 W and the MAPE was 8.6 ± 1.5%. For P3, the corresponding values were 79.2 ± 30.5 W and 10.6 ± 3.3%, respectively.

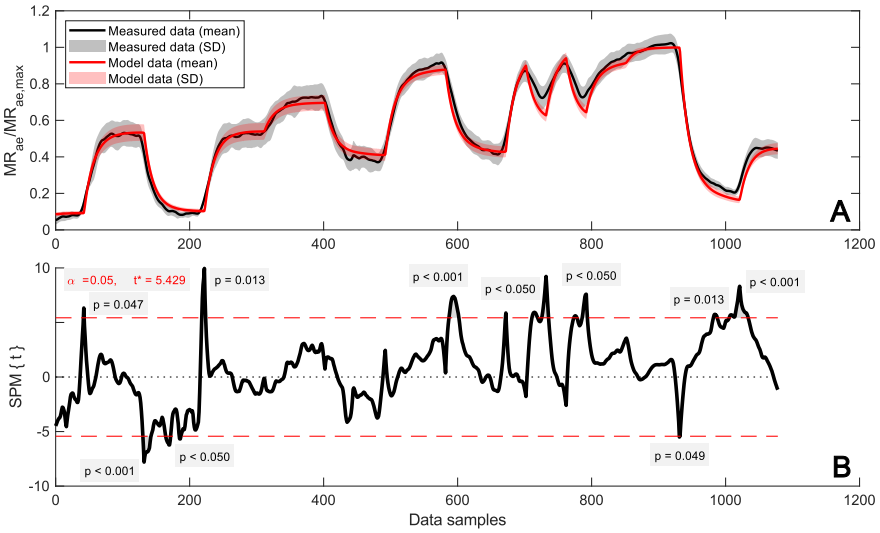

Figure 10. Time resolved mean and SD (Panel A) and statistical parametric mapping from the two-tailed paired t-test (Panel B) of measured and modeled MR_{ae} normalized with $MR_{ae,max}$ for P3 (n=11). Results from three subjects are omitted due to deviations in duration during one or more periods (same subjects as in Figure 9). Data for the period leading to volitional exhaustion has been stretched/squeezed to allow averaging across the subjects. The dashed lines show the critical t-value, indicating the limit for significant differences (P < 0.05) between measured and modeled data.

From the parameter estimation, the mean values of A_{ve} and A_{acc} were 11.0% and 6.9% of $MR_{ae,max}$ respectively, and the mean values of MR_{rest}, MR_{lt}, and $MR_{ae,max}$ was 105.9%, 99.2%, and 98.5% of their respective approximations from measurements. The mean value of τ_{ae} and τ_{la} was 25.8 s and 12.9 s, respectively. The mean alactic system capacity ($E_{al,max}$) was 16.3 kJ.

The mean $MR_{ae}/MR_{ae,max}$ shows an overall good agreement between model and measurement for both P2 (Figure 9) and P3 (Figure 10), but in the same figures the SPMs show significant differences in several sections of the protocols. The data for a representative subject (Figure 11) show that the model fails to capture the measured MR_{ae} especially during relatively lower intensity exertion following higher intensity

exertion. Also, during the highest intensity leading up to exhaustion, measured MR_{ae} is closer to linear and this neither is captured by the model.

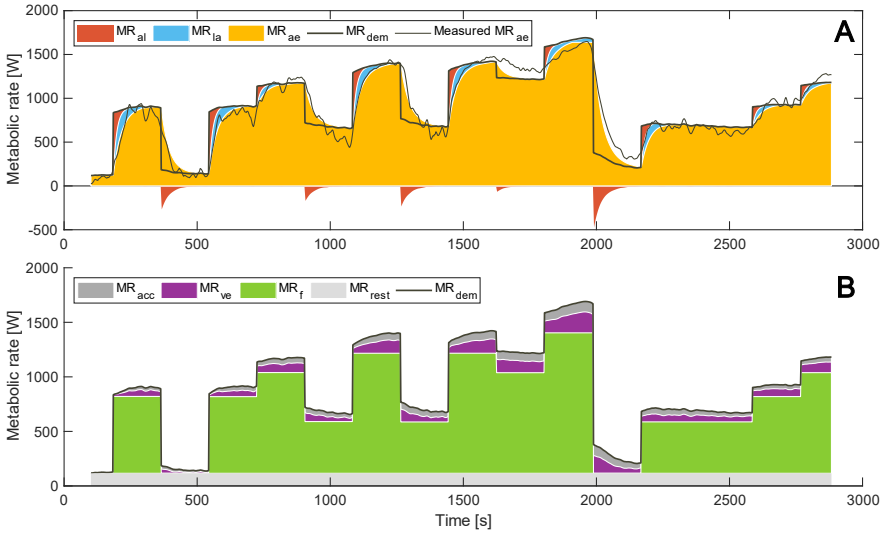

Figure 11. Metabolic supply rates (Panel A) and metabolic demand rates (Panel B) for P2 in a representative subject (S8). MR_{al} is alactic metabolic rate, MR_{la} lactic metabolic rate, MR_{ae} modeled aerobic metabolic rate, MR_{dem} total metabolic demand rate and measured MR_{ae} measured aerobic metabolic rate (Panel A). MR_{acc} is metabolic demand rate due to accumulated metabolites, MR_{ve} metabolic demand rate due to ventilation, MR_f metabolic demand rate due to the fundamental work and MR_{rest} the metabolic demand rate at rest. In Panel A MR_{rest} is included in MR_{ae}.

5.4.5 Conclusions

The MAPE of 10.6% in P3 is in line with the results of Artiga Gonzalez et al. (2019). The proposed model shows good overall agreement with measurements but fails to capture certain aspects. Especially, many of the recovery periods show lower agreement. Even though a typical slow component is not visible in the data, the last two bouts leading up to exhaustion are not captured as well. Furthermore, the $[mLa^-]/V_m$ reaches above 1 for most subjects in P3 which is infeasible by model

definition and reveal the fatiguing aspects of the model need improvement.

The use of $\dot{V}_E$ as independent variable was judged as needed to avoid too much unreliability, but for application purposes it would be desirable to use ergometer power as the sole input to the model.

Still, the proposed model is a step towards understanding the behavior of the human bioenergetic system. With the more distinct periods of recovery included in P2 and P3, the Margaria-Morton model would likely yield unreasonable results, since the full difference between MR_{dem} and MR_{ae} during recovery will be credited the anaerobic systems. In the proposed model this is countered in part by introducing MR_{ve} and MR_{acc} which increases MR_{dem} during recovery, and in part by introducing an alactic recovery efficiency of about 41%.

6 Overall discussion and conclusions

The results from this thesis highlight the relative simplicity of performing numerical simulations of endurance sports with a propulsive power model. This approach effectively quantifies the impact from dynamic friction on race times in cross-country skiing under specified conditions. To obtain knowledge about this kind of equipment-to-environment or in some cases athlete-to-environment interactions, the group mean input from a propulsive power model may be sufficient and should be used in favor of simplicity.

The thesis does not show the full complexity of performing numerical simulations with a bioenergetic model as a restriction of the athlete's power output, as it focuses on the development and validation of bioenergetic models. But the mere comparison of the formulations (propulsive power model to bioenergetic model) is an indication of the complexity. Still, there are numerous possible applications from this more complex approach. The proposed bioenergetic model in Paper III attempts to describe the dynamic behavior in known metabolic systems and metabolic processes contributing to the total metabolic demand. Part of the energy supply formulation, including several metabolic demand processes and connecting part of the metabolic energy supply systems to the energy demanding processes offers a new approach on the modeling compared to earlier attempts (Morton, 1990; Sundström, 2016). The close relation to the known human physiology means that the model parameters can be viewed as determinants of performance – many of which are new determinants not considered before. Additionally, in both Paper II and III non-linear grey-box parameter estimation was used to successfully individualize the bioenergetic models to reflect specific athletes. With repeated testing and individualization of the proposed

bioenergetic model (or future developments) for the same athletes, more knowledge can be gained about these new determinants, their impact on performance and how to improve them most effectively. This could lead to better knowledge about the abilities and restriction in human physiology and more well adapted individual training programs with higher impact on performance and lower risk of injury or overtraining.

In Paper II the smallest median RMSE of MR_{ae} between model and measurement when fitted to STT1 data was 50.0 W and 77.6 W when applied to STT2 with an estimated median $MR_{ae,max}$ (M_{O2}) of 1.75 kW. In Paper III the mean RMSE when fitted to P2 was 61.9 W and 79.2 W when applied to P3 with an estimated mean $MR_{ae,max}$ of 1.65 kW. The results are of comparable magnitude even though the comparison of models between the studies is clouded by differences in test-retest variations and test protocol design. Investigations of the time-series data in both Paper II and III showed a RMSE of this magnitude indicate an overall good fit but with losses in finer details. The proposed model can be used as a restriction for optimizing pacing strategies (metabolic power distribution during a race) or predicting race performance, but one must be cautious when applying the model to a different protocol (or racecourse) than the one used during the parameter estimation. It is desirable to further development the model to reduce the RMSE and capture more details. This would strengthen the reliability in both the predicting ability and usefulness of the new determinants (model parameters). It should be noted that e.g., a black-box model trained with a neural network might result in a lower RMSE, but this would be at the price of loosing the close connection and thereby understanding of the human bioenergetic

system. This in turn would make it more difficult to assess the reliability when applying the model to different protocols.

In summary, the results from this thesis show the relative simplicity of performing numerical simulations with a propulsive power model, the increased complexity that comes with using a bioenergetic model instead and argue for the benefits of both approaches. Furthermore, the thesis makes recognizable contributions to establish non-linear grey-box parameter estimation as a reliable method of individually adapting bioenergetic models. Paper II and III constitute two out of three known contributions (the first being Artiga Gonzalez et al. (2019)) where this method was used and all studies proved successful in the parameter estimation. Finally, the newly developed bioenergetic model is a notable step towards better understanding and improving predictions of the behavior of the human bioenergetic system.

7 Future research

Most numerical simulations with propulsive power models (including Paper I) communicate the results as if they were an exact truth. By including and making Monte Carlo simulations a requirement in such numerical simulations, the distributions of included parameters could be used to generate a simulation grid which in turn would yield results in terms of mean and standard deviation as well as allowing statistical hypothesis testing. Due to higher computational demand, this might not yet be feasible when using bioenergetic modeling.

The method of parameter estimation has proven efficient in providing well-adapted solutions, but the utilized multi-start global optimization method is the simplest method. Employing a more efficient method could either save computational time or reduce the risk of missing a global optimum by performing more relevant local grey-box parameter estimations.

The developed bioenergetic model show great potential but clearly also fails in certain aspects. Further research is needed to reach an even better understanding and improved prediction of the behavior of the human bioenergetic system. Possible modeling ideas to explore could be to separate the complete glycolytic system from the purely oxidative system and/or include separate formulations for the muscle lactate and blood lactate concentrations. Additionally, quantifying the contribution of different processes in the human body to the total metabolic demand rate would be extremely useful when improving the bioenergetic models.

8 References

Andersson, E., Björklund, G., Holmberg, H.-C., and Ørtenblad, N. (2017). Energy system contributions and determinants of performance in sprint cross-country skiing. *Scandinavian Journal of Medicine & Science in Sports* 27, 385–398. doi:10.1111/sms.12666.

Artiga Gonzalez, A., Bertschinger, R., Brosda, F., Dahmen, T., Thumm, P., and Saupe, D. (2019). Kinetic analysis of oxygen dynamics under a variable work rate. *Human Movement Science* 66, 645–658. doi:10.1016/j.humov.2017.08.020.

Atkinson, G., Peacock, O., and Passfield, L. (2007). Variable versus constant power strategies during cycling time-trials: Prediction of time savings using an up-to-date mathematical model. *J Sport Sci* 25, 1001–1009. doi:10.1080/02640410600944709.

Budde, R., and Himes, A. (2017). High-resolution friction measurements of cross-country ski bases on snow. *Sports Engineering* 20, 299–311. doi:10.1007/s12283-017-0230-5.

Carlsson, P., Tinnsten, M., and Ainegren, M. (2011). Numerical simulation of cross-country skiing. *Comput Method Biomec* 14, 741–6. doi:10.1080/10255842.2010.493885.

Ferguson, C., Rossiter, H. B., Whipp, B. J., Cathcart, A. J., Murgatroyd, S. R., and Ward, S. A. (2010). Effect of recovery duration from prior exhaustive exercise on the parameters of the power-duration relationship. *J Appl Physiol (1985)* 108, 866–874. doi:10.1152/japplphysiol.91425.2008.

Gaesser, G. A., and Brooks, G. A. (1984). Metabolic bases of excess post-exercise oxygen consumption: a review. *Med Sci Sports Exerc* 16, 29–43.

Gløersen, Ø., Gilgien, M., Dysthe, D. K., Malthe-Sørenssen, A., and Losnegard, T. (2020). Oxygen demand, uptake, and deficits in elite cross-country skiers during a 15-km race. *Med Sci Sports Exerc* 52, 983–992. doi:10.1249/MSS.0000000000002209.

Gløersen, Ø., Losnegard, T., Malthe-Sørenssen, A., Dysthe, D. K., and Gilgien, M. (2018). Propulsive Power in Cross-Country Skiing: Application and Limitations of a Novel Wearable Sensor-Based Method During Roller Skiing. *Front. Physiol.* 9. doi:10.3389/fphys.2018.01631.

Margaria, R. (1976). *Biomechanics and energetics of muscular exercise*. Clarendon Press Oxford.

McArdle, W. D., Katch, F. I., and Katch, V. L. (2009). *Exercise Physiology: Nutrition, Energy, and Human Performance*. 7th edition. Philadelphia: Lippincott Williams & Wilkins.

Monod, H., and Scherrer, J. (1965). The work capacity of a synergic muscular group. *Ergonomics* 8, 329–338. doi:10.1080/00140136508930810.

Moritani, T., Nagata, A., deVries, H. A., and Muro, M. (1981). Critical power as a measure of physical work capacity and anaerobic threshold. *Ergonomics* 24, 339–350. doi:10.1080/00140138108924856.

Morton, R. H. (1986). A three component model of human bioenergetics. *J. Math. Biol.* 24, 451–466. doi:10.1007/BF01236892.

Morton, R. H. (1990). Modelling human power and endurance. *J. Math. Biol.* 28, 49–64. doi:10.1007/BF00171518.

Morton, R. H. (2006). The critical power and related whole-body bioenergetic models. *Eur J Appl Physiol* 96, 339–354. doi:10.1007/s00421-005-0088-2.

Morton, R. H., and Billat, L. V. (2004). The critical power model for intermittent exercise. *Eur J Appl Physiol* 91, 303–307. doi:10.1007/s00421-003-0987-z.

Moxnes, J. F., Sandbakk, Ø., and Hausken, K. (2014). Using the power balance model to simulate cross-country skiing on varying terrain. *Open Access J Sports Med* 5, 89–98. doi:10.2147/OAJSM.S53503.

Poole, D. C., and Jones, A. M. (2012). Oxygen uptake kinetics. *Comprehensive Physiology* 2, 933–996. doi:10.1002/cphy.c100072.

Skiba, P. F., Chidnok, W., Vanhatalo, A., and Jones, A. M. (2012). Modeling the expenditure and reconstitution of work capacity above critical power. *Med Sci Sports Exerc* 44, 1526–1532. doi:10.1249/MSS.0b013e3182517a80.

Skiba, P. F., Fulford, J., Clarke, D. C., Vanhatalo, A., and Jones, A. M. (2015). Intramuscular determinants of the ability to recover work capacity above critical power. *Eur J Appl Physiol* 115, 703–713. doi:10.1007/s00421-014-3050-3.

Stirling, J. R., Zakynthinaki, M. S., and Saltin, B. (2005). A model of oxygen uptake kinetics in response to exercise: Including a means of calculating oxygen demand/deficit/debt. *Bulletin of Mathematical Biology* 67, 989–1015. doi:10.1016/j.bulm.2004.12.005.

Sundström, D. (2016). On a bioenergetic four-compartment model for human exercise. *Sports eng* 19, 251–263. doi:10.1007/s12283-016-0205-y.

Sundström, D., and Bäckström, M. (2017). Optimization of pacing strategies for variable wind conditions in road cycling. *Proceedings of the Institution of Mechanical Engineers, Part P: Journal of Sports Engineering and Technology* 231, 184–199. doi:10.1177/1754337117700550.

Sundström, D., Carlsson, P., Ståhl, F., and Tinnsten, M. (2013). Numerical optimization of pacing strategy in cross-country skiing. *Struct Multidisc Optim* 47, 943–950. doi:10.1007/s00158-012-0856-7.

Swain, D. P. (1997). A model for optimizing cycling performance by varying power on hills and in wind. *Med Sci Sport Exer* 29, 1104–8. doi:10.1097/00005768-199708000-00017.

Vella, C. A., Marks, D., and Robergs, R. A. (2006). Oxygen cost of ventilation during incremental exercise to VO2 max. *Respirology* 11, 175–181. doi:10.1111/j.1440-1843.2006.00825.x.

Wolf, S., and Saupe, D. (2017). How to Stay Ahead of the Pack: Optimal Road Cycling Strategies for two Cooperating Riders. *Int J Comp Sci Sport* 16, 88–100. doi:10.1515/ijcss-2017-0008.